Flexural buckling of concrete-filled aluminium alloy CHS columns: Numerical modelling and design

Evangelia Georgantzia, Michaela Gkantou

School of Civil Engineering and Built Environment, Faculty of Engineering and Technology, Liverpool John Moores University, L3 3AF, Emails: e.georgantzia@ljmu.ac.uk; m.gkantou@ljmu.ac.uk

Abstract. The current study deals with numerical modelling and design framework of concrete-filled aluminium alloy columns with circular hollow sections (CHSs) under pin-ended boundary conditions. The examined aluminium alloy is 6082-T6 and the concrete infill has cylinder compressive strength of 30 MPa. Finite element modelling was employed to simulate the investigated columns. Reported test data were used to verify the developed finite elements models. Material and geometrical non-linearities were considered during the analyses. Parametric analyses have been executed to generate structural performance results over a wide range of member slenderness for a stocky and a slender cross-section. The obtained load-mid-height lateral displacement curves were discussed. The ultimate capacities predicted by numerical analyses were utilised to assess the design strengths predicted using combined formulae of EN 1994-1-1 and EN 1999-1-1 and design criteria proposed by Zhou and Young for the plastic resistance of concrete-filled aluminium alloy CHS combined with flexural buckling strength predictions suggested by EN 1999-1-1. It was shown that the latter provides more accurate and consistent design strength predictions.

Keywords: Flexural buckling; Aluminium alloys; Concrete-filled; Circular Hollow Sections; Numerical Modelling; Design Predictions.

1. Introduction

In recent years aluminium alloys have been widely employed as structural materials in a variety of applications including high-rise buildings, sport facilities, footbridges and pavilions. Their inherent advantageous features, such as ease of fabrication, great strength-to-weight ratio, high recyclability, prominent resistance against corrosion and aesthetic appearance have contributed to their growing popularity among structural engineers and architects. A design consideration is the limited stiffness exhibited by the aluminium alloy structural members that is related to their low Young's Modulus which is three times lower than that of steel. However, in case of tubular structures, filling the aluminium alloy tubes with concrete could significantly enhance the strength and stiffness of the members.

Adopting similar principles with the concrete-filled steel tubes (CFST), this paper investigates the potential of using aluminium alloy tubular members combined with concrete. Zhou & Young [1,2] tested concrete-filled aluminium alloy stub columns with square hollow sections (SHSs), rectangular hollow sections (RHSs) and circular hollow sections (CHSs) under axial compression and found that the AS/NZS 1664.1 [3] and AA 2020 [4] design specifications are generally conservative. Moreover, Zhou & Young [5] proposed design formulae for concrete-filled aluminium alloy CHSs considering the benefits of material interaction due to confinement. In another study, Zhou & Young [6] evaluated through testing the structural performance of concrete-filled double-skin tubes against axial compressive loading. Wang et al. [7] utilised the reported data [1] and assessed whether the "nominal yield strength" method available in GB 50936 [8] for CFST could be applied to concrete-filled aluminium tubular (CFAT) members, finding that the design predictions are conservative but reliable. Recently, Georgantzia et al. [9] reported the experimental results on flexural buckling response of SHSs and RHSs CFAT columns. The aforementioned experimental and numerical studies demonstrated the high capability of this type of composite members used in structural applications.

However, research work on flexural buckling response of aluminium alloy CHS slender columns infilled with concrete still remains scarce. The present study aims to investigate numerically the flexural buckling response of slender CFAT columns with CHSs and pin-ended support conditions. Finite element modelling was employed to simulate the examined columns using the commercially available software package Abaqus [10]. The material modelling of confined concrete and the interaction properties of the aluminium tube/concrete infill interface were carefully considered. The experimental data reported by [9] were utilised to assess the accuracy of the developed finite element (FE) models. Subsequently, a series of parametric analyses was performed to generate structural performance results for concrete-filled aluminium alloy CHS columns including different thicknesses and a wide range of member slenderness. Finally, the numerically obtained column capacities were used to evaluate the design predictions using the European standards [11,12] and design criteria proposed by Zhou and Young [5].

2. Numerical Modelling

2.1 Modelling assumptions

The commercially available software package Abaqus [10] was employed to develop the three-dimensional finite element (FE) models. First order continuum hexahedral elements (C3D8R) with reduced integration and hourglass behaviour control were adopted as more suitable to deal with material and geometrical non-linearities. Following a mesh convergence study, an element size of 5 mm and minimum three elements across the plate thickness of the aluminium tube was found to provide the optimum combination of accuracy and computational efficiency.

An elastic-plastic material model with linear isotropic hardening was adopted to describe the behaviour of the aluminium alloy tubes. The Poisson's ratio was defined as 0.33. To consider the material plasticity, the average engineering stress-strain curves (Fig. 1(a)) reported by Georgantzia et al. [9] were utilised and converted into true stress-strain values.

In line with past studies [13-15], the inelastic behaviour of concrete was modelled employing the concrete damaged plasticity model available in Abaqus [10]. The flow potential eccentricity and the viscosity parameter were defined equal to 0.1 and 0, accordingly. The dilation angle was calculated according to Tao et al. [15] for circular sections considering the confinement effect. Furthermore, the Poisson's ratio was adopted equal to 0.2, whereas the Young's Modulus was determined by the empirical relationship suggested in EN 1992-1-1 [16]. The ratio of the second stress invariant on the tensile meridian over that on the compressive meridian and the ratio of the compressive strength under biaxial loading over uniaxial compressive strength were defined in line with [17] and [18], respectively. Linear tensile behaviour of concrete infill was assumed up to maximum tensile strength equal to 10% of the cylinder compressive strength [16]. Beyond this point, the concrete's tension softening behaviour was described using the stress-crack opening displacement relationship reported by [19] accounting for the fracture energy according to [20,21].

When a CFAT column is subjected to axial compression, the concrete infill expands laterally and it is confined passively by the aluminium tube. This mechanism results in significant increase on the strength and ductility of the specimen. It is anticipated that the concrete infill under confinement pressure exhibits similar behaviour with the corresponding one confined by a steel tube [2]. Consequently, a three-stage model (OA, AB, BC) for confined concrete proposed for CFST columns [15] was adopted herein for the concrete infill (Fig. 1(b)).

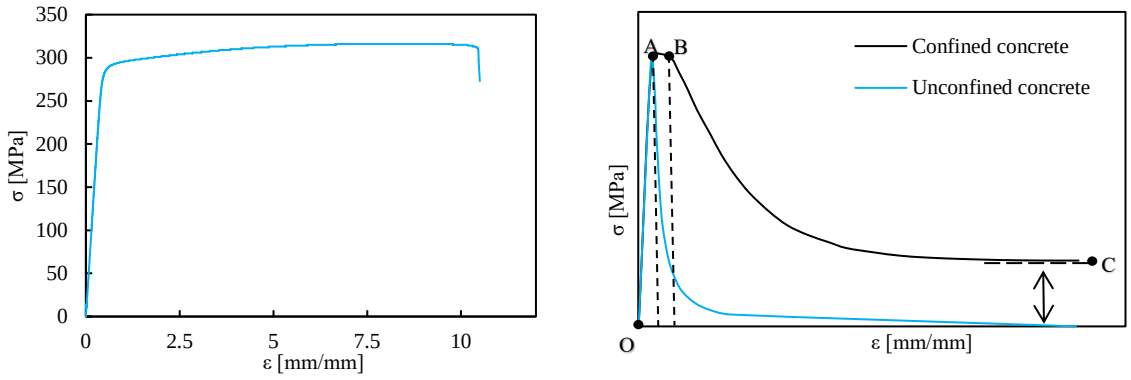

(a) aluminium alloy [9] (b) concrete infill [15]

Fig. 1. Material properties adopted in the FE.

The interaction properties of the aluminium tube/concrete infill interface were defined through surface-to-surface contact. In the normal direction "Hard contact" was employed which allows for separation of the surfaces in tension and prevents from penetration in compression. In tangential direction the behaviour was represented by the Coulomb friction model. In line with past studies on CFST columns [22], a value of 0.3 was considered for the friction coefficient.

Initial geometric imperfections generated during fabrication process and handling significantly influence the buckling behaviour of a column and therefore should be considered in the FE modelling. To do so, an initial linear buckling analysis was executed and the lowest buckling mode was superposed onto the initial perfect geometry with an amplitude of $L/1000$, where L is the column length, in line with EN 1999-1-1 [12]. Local geometric imperfections were not explicitly considered, as their effect is restrained by the concrete infill.

Taking advantage of symmetry in geometry, boundary conditions and applied loads the half of the specimen was modelled implementing suitable boundary conditions on the symmetry plane. The bottom and top edges of the column were tied with two reference points using kinematic coupling constraints, as illustrated in Fig. 2. All degrees of freedom were restrained except from the rotation around the buckling axis at both reference points (RP) and the translation along the member length at the top reference point. A concentrated displacement was applied on the top reference point and a non-linear static analysis using Riks solution method [10] was carried-out to obtain the full-range of the load-mid-height lateral displacement curves. It should be mentioned that in the present study, the examined aluminium alloy profiles are considered as heat-treated and extruded and thus the residual stresses were not explicitly modelled [23-25].

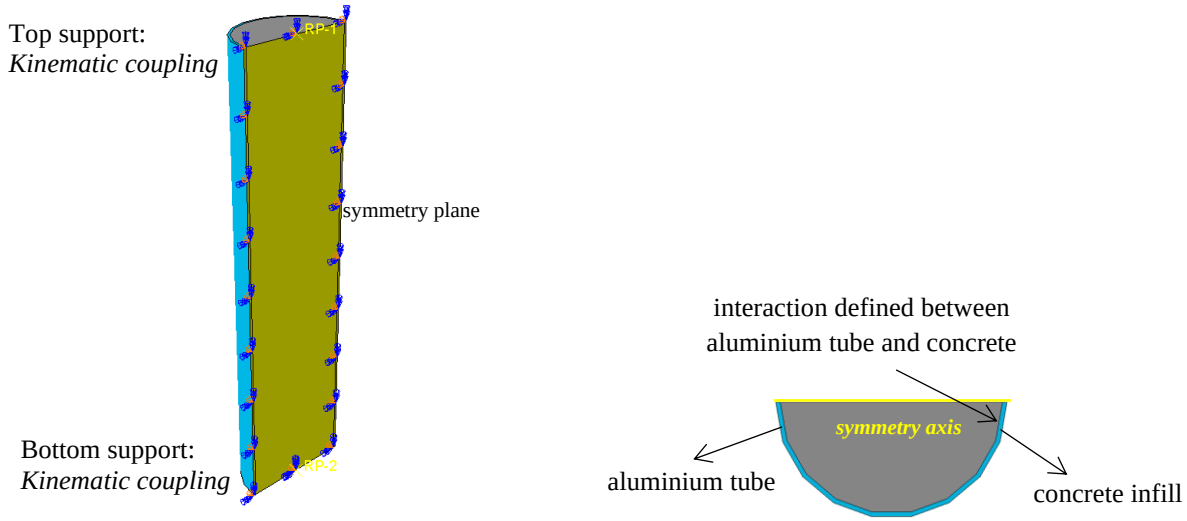

Fig. 2. Geometrical modelling and applied boundary conditions.

2.2 Model validation

In absence of experimental data on concrete-filled CHS slender columns, the experimental programme reported by Georgantzia et al. [9] on SHS and RHS CFAT columns was used to verify the accuracy of the developed FE models. Figs. 3(a) and 3(b) illustrate the load-mid-height lateral displacement curves for a typical specimen obtained from test and finite element analysis (FEA) and the corresponding failure modes, respectively. As can be observed, a good convergence has been achieved between the experimental and numerical response. Moreover, the failure modes predicted by the FEA was found to be in line with the corresponding experimental ones. Hence, it is assumed that the developed FE models are able to accurately capture the buckling response of CFAT columns

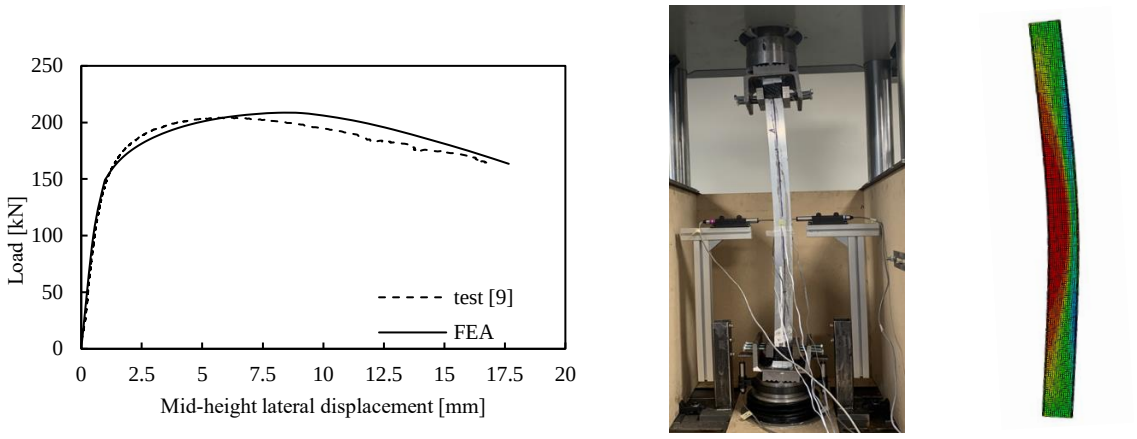

(a) Load-mid-height lateral displacement curves (b) Flexural buckling failure mode

Fig. 3. Comparison of experimental [9] and numerical results.

3. Parametric study

A series of parametric analyses were executed on the basis of the validated FE models to determine the effect of the thickness and member slenderness on the buckling resistance of circular CFAT columns. A series of 26 FE models were examined with 100 mm constant outer diameter (D) and two different thicknesses (t) of 2 and 10 mm. Note that the aluminium tube with thickness 2 mm is a slender cross-section and explicit allowances should be made to consider the effects of local buckling when calculating the cross-sectional resistance, while the section with thickness 10 mm is a stocky cross-section and can attain the yield load. The specimens' length (L) was ranging from 400 to 2600 mm covering a wide range of member slenderness ($\bar{\lambda}$) [12]. Cylinder compressive strength of 30 MPa was defined for the concrete infill. The specimens were labelled according to their geometrical properties. For example, "100×2-400" indicates that the investigated column comprises of aluminium tube with 100 mm diameter and thickness of 2 mm and its length is equal to 400 mm. The specimen designation and the geometric dimensions are presented in Table 1.

According to the FE results, all specimens failed due to flexural buckling. Fig. 4(a) presents the load versus mid-height lateral displacement curves for two typical specimens obtained from the parametric study. As expected the ultimate capacity is higher for specimens with thicker aluminium tubes. This stems from the fact that as the thickness of the aluminium tube increases, the stiffness of the specimen increases as well, improving the resistance against buckling failure. Fig.4 (b) illustrates the load versus mid-height lateral displacement curves for specimens with same cross-section but different lengths. As can be seen longer columns characterised by higher member slenderness ($\bar{\lambda}$) are more prone to flexural buckling and thus the ultimate capacity is decreased.

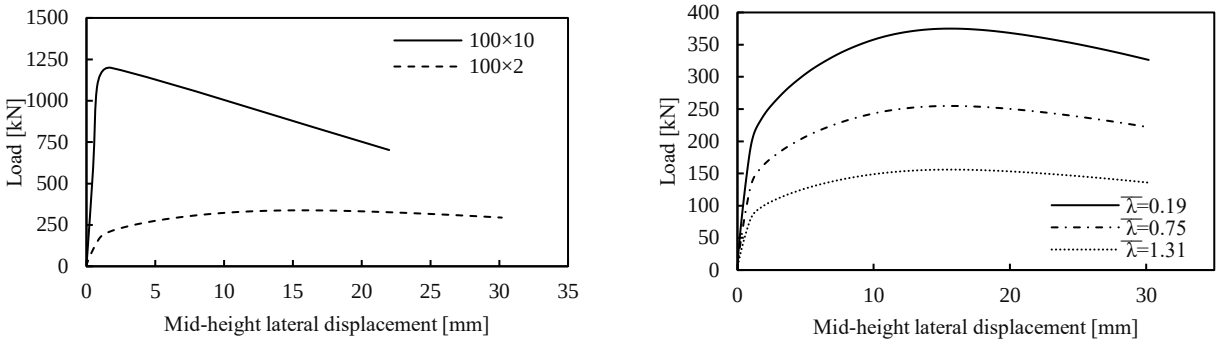

(a) L=1000 mm (b) 100×2

Fig. 4. Typical load-mid-height lateral displacement curves from FE studies.

Table 1. Geometrical properties and results obtained from parametric study.

Specimen	D [mm]	t [mm]	L [mm]	D/t	$\bar{\lambda}$	N_{FEA}	$N_{FEA}/N_{EC4,EC9}$	$N_{FEA}/N_{Zhou\&Young,EC9}$
100×2-400	100	2	400	50	0.19	454.92	1.19	1.22
100×10-400	100	10	400	10	0.26	1374.80	1.32	1.05
100×2-600	100	2	600	50	0.28	441.24	1.31	1.20
100×10-600	100	10	600	10	0.39	1375.07	1.48	1.08
100×2-800	100	2	800	50	0.37	436.13	1.43	1.22
100×10-800	100	10	800	10	0.52	1275.85	1.46	1.05
100×2-1000	100	2	1000	50	0.47	410.16	1.43	1.18
100×10-1000	100	10	1000	10	0.65	1198.43	1.44	1.04
100×2-1200	100	2	1200	50	0.56	364.41	1.45	1.08
100×10-1200	100	10	1200	10	0.78	1079.23	1.40	1.01
100×2-1400	100	2	1400	50	0.65	330.06	1.37	1.02
100×10-1400	100	10	1400	10	0.91	991.41	1.43	1.02
100×2-1600	100	2	1600	50	0.75	309.18	1.35	1.00
100×10-1600	100	10	1600	10	1.04	870.01	1.43	1.02
100×2-1800	100	2	1800	50	0.84	291.73	1.36	1.01
100×10-1800	100	10	1800	10	1.18	762.16	1.45	1.04
100×2-2000	100	2	2000	50	0.94	275.83	1.39	1.04
100×10-2000	100	10	2000	10	1.31	677.66	1.50	1.08
100×2-2200	100	2	2200	50	1.03	255.89	1.42	1.06
100×10-2200	100	10	2200	10	1.44	555.37	1.43	1.03
100×2-2400	100	2	2400	50	1.12	224.83	1.38	1.03
100×10-2400	100	10	2400	10	1.57	467.13	1.39	1.00
100×2-2600	100	2	2600	50	1.22	207.07	1.42	1.06
100×10-2600	100	10	2600	10	1.70	435.02	1.49	1.07
100×2-2800	100	2	2800	50	1.31	189.25	1.45	1.08
100×10-2800	100	10	2800	10	1.83	389.12	1.52	1.09
mean							**1.41**	**1.07**
COV							**0.05**	**0.06**

4. Assessment of strength predictions

European codes do not provide stability design criteria for composite aluminium-concrete structural members. Therefore, the present study adopts and assesses the design formulae for composite steel-concrete structures available in EN 1994-1-1 [11] replacing the material properties of steel with the corresponding ones of the examined aluminium alloy in line with EN 1999-1-1 [12]. The design equations proposed by Zhou & Young [5] for the plastic resistance of circular concrete-filled hollow sections are, also, assessed herein. In both design methodologies the contribution of the confinement effect on the plastic resistance of the column is considered. Table 1 presents the column strengths resulted from the parametric study (N_{FEA}) and the comparison with those calculated by the combined formulae of EN 1994-1-1 ($N_{EC4,EC9}$) for the cross-sectional resistance and EN 1999-1-1 for the buckling strength. In addition, the proposed design equations by Zhou & Young ($N_{Zhou\&Young,EC9}$) combined with EN 1999-1-1 are assessed. The mean value and the corresponding coefficient of variation (COV) of $N_{FEA}/N_{EC4,EC9}$ is 1.41 and 0.05 respectively, whilst for $N_{FEA}/N_{Zhou\&Young,EC9}$ are 1.07 and 0.06 respectively. It can be observed that the design predictions in both cases are lower than the corresponding obtained by FEA which suggests that are safe but conservative. Low values of COVs indicate that the predictions are consistent. The same can be observed by Fig. 5(a), where the numerically obtained capacities (N_{FEA}) over the predicted (N_{pred}) ones are plotted against the member slenderness ($\bar{\lambda}$) of the columns. All values are higher than unity which suggests safety. Comparing the two methodologies it can be extracted that the predicted column strengths using the suggested formulae by Zhou & Young are more accurate as they are closer to unity. The same conclusions can be reached by Fig. 5(b), where the ultimate capacities (N_{FEA}) normalised by the plastic resistances ($N_{pl,Rk,EC4,}$ $N_{pl,Rk,Zhu\&Young}$) are plotted against ($\bar{\lambda}$). The Eurocode buckling design curve [12] is also plotted in the same figure. Again it can be seen that the design predictions are safe and consistent, but the formulae suggested by Zhou & Young provide improved design accuracy.

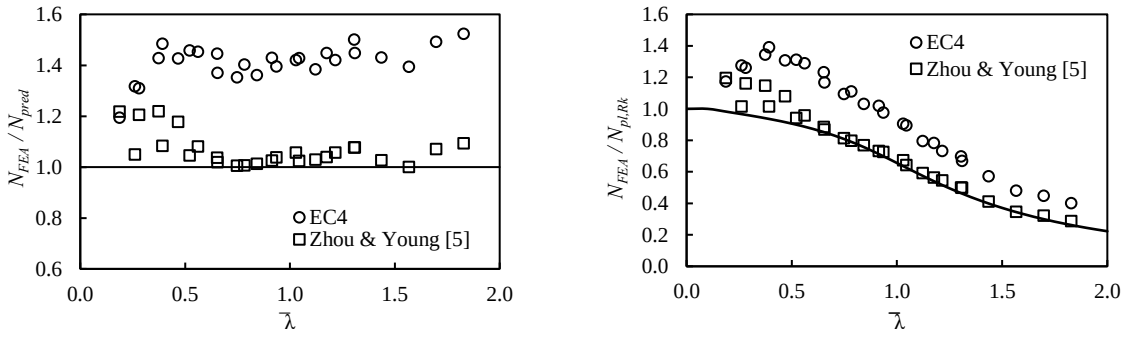

(a) N_{FEA}/N_{pred} (b) $N_{FEA}/N_{pl,Rk}$

Fig. 5. Comparison of FE results with design columns strengths.

5. Conclusions

The current study presents detailed numerical modelling of aluminium alloy circular hollow section columns infilled with concrete. Constitutive material properties of confined concrete and geometrical imperfections were considered during the analyses. Experimental data reported in literature were utilised to evaluate the precision degree of the developed FE models. Upon validation, parametric analyses were executed and generated results on structural response over a wide range of member slenderness for a stocky and a slender cross-section. Following, the obtained capacities were used to assess the buckling strength predictions using combined formulae of EN 1994-1-1 and EN 1999-1-1 and combined formulae of Zhou and Young and EN 1999-1-1. It was concluded that in both cases the design predictions are safe and consistent. Furthermore, the design equations proposed by Zhou and Young for the cross-sectional plastic resistance were found to be more accurate. Overall, further investigation is suggested so that to extend the pool of performance data of concrete-filled aluminium alloy columns for a more extensive range of alloys and cross-sections.

Acknowledgements

The financial support of the Faculty of Engineering and Technology of Liverpool John Moores University is gratefully acknowledged.

References

1. Zhou F, Young B (2008) Tests of concrete-filled aluminum stub columns. Thin-Walled Structures, 46(6), pp.573–83.
2. Zhou F, Young B (2009) Concrete-filled aluminum circular hollow section column tests. Thin-Walled Structures, 47(11), pp.1272–1280.
3. Australian/New Zealand Standard (AS/NZS) (1997) Aluminium structures part 1: Limit state design. AS/NZS 1664.1:1997. Standards Australia, Sydney, Australia.
4. The Aluminum Association (2000) Aluminum Design Manual. Washington, D.C.
5. Zhou F, Young B (2012) Numerical analysis and design of concrete-filled aluminum circular hollow section columns. Thin-Walled Structures, 50, pp.45–55.
6. Zhou F, Young B (2018) Concrete- filled double-skin aluminum circular hollow section stub columns. Thin-Walled Structures, 133, pp.141–52.
7. Wang F, Zhao H, Han L (2019) Analytical behavior of concrete-filled aluminum tubular stub columns under axial compression. Thin-Walled Structures, 140, pp.21–30.
8. GB 50936-2014 (2014) Technical code for concrete filled steel tubular structures.
9. Georgantzia E, Bin Ali S, Gkantou M, Kamaris GS, Kansara K, Atherton W (2021) Structural response of aluminium alloy concrete filled tubular columns. In: Eurosteel. Sheffield, United Kingdom. 1-3 September 2021 (Accepted)
10. Abaqus (2018) Abaqus Standard User's Manual. Version 2016. Provid RI Dassault Syst Corp.
11. European Committee for Standardisation (EC4) (2004) Eurocode 4: Design of Composite Steel and Concrete Structures. Part 1-1: General Rules and Rules for Buildings. BS EN 1994-1-1: 2004. CEN: 2004. BSI.
12. European Committee for Standardisation (EC9) (2007) Eurocode 9: Design of aluminium structures. Part 1-1: General structural rules - General structural rules and rules for buildings. BS 1999-1-1:2007+A2:2013, CEN: 2007. BSI.
13. Tziavos NI, Gkantou M, Theofanous M, Dirar S, Baniotopoulos C (2020) Behaviour of grout-filled double-skin tubular steel stub-columns: Numerical modelling and design considerations. Structures, 27, pp.1623-1636.
14. Gkantou M, Theofanous M, Baniotopoulos C (2020) A numerical study of prestressed high strength steel tubular members. Frontiers of Structural and Civil Engineering, 14(1), pp.10-22.
15. Tao Z, Wang Z Bin, Yu Q (2013) Finite element modelling of concrete-filled steel stub columns under axial compression. Journal of Constructional Steel Research, 89, pp.121–31.
16. European Committee for Standardisation (EC2) (2004) Eurocode 2: Design of Concrete Structures. Part 1-1: General rules and rules for buildings. BS EN 1992-1-1: CEN: 2004. BSI.
17. Papanikolaou VK, Kappos AJ (2007) Confinement-sensitive plasticity constitutive model for concrete in triaxial compression International Journal of Solids and Structures, 44(21), pp.7021–48.
18. Yu T, Teng JG, Wong YL, Dong S (2010) Finite element modelling of confined concrete-I: Drucker-Prager type plasticity model. Engineering Structures, 32(3), pp.665–79.
19. Hordijk D (1991) Local approach to fatigue of concrete. Ph D thesis Delft Univ Technol Delft, Netherlands.
20. FIP (1993) Ceb-Fip Model Code 1990. Ceb-Fip Model Code 1990.
21. Bažant Z, Becq-Giraudon E (2002) Statistical prediction of fracture parameters of concrete and implications for choice of testing standard. Cement Concrete Research, 32(4), pp.529–556.
22. Lam D, Dai XH, Han LH, Ren QX, Li W (2012) Behaviour of inclined, tapered and STS square CFST stub columns subjected to axial load. Thin-Walled Structures, 54, pp.94–105.
23. Mazzolani FM (1975) Residual Stress Tests Alu-Alloy Austrian Profiles, ECCS Committee, Brussels, Technical Report, Doc 16-75-1.
24. Fenga R, Liu J (2019) Numerical investigation and design of perforated aluminium alloy SHS and RHS columns. Engineering Structures, 199, pp.109591.

25. Georgantzia E, Gkantou M and Kamaris GS (2021) Aluminium alloys as structural material: A review of research. Engineering Structures, 227. pp.111372.